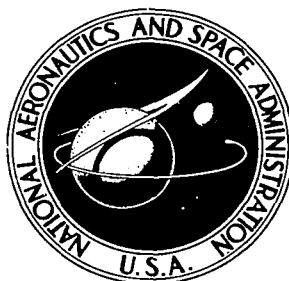


NASA TECHNICAL NOTE

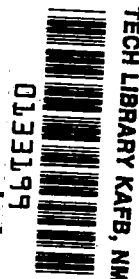


NASA TN D-6607

c. 1

NASA TN D-6607

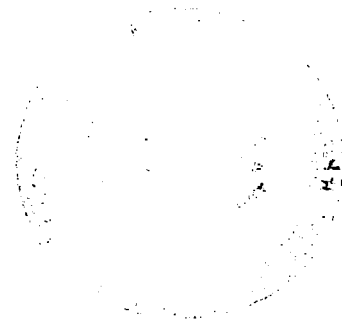
LOAN COPY: RET  
AFWL (DOU  
KIRTLAND AFB,



PREDICTED CHARACTERISTICS  
OF AN OPTIMIZED SERIES-HYBRID  
CONICAL HYDROSTATIC BALL BEARING

*by Lester J. Nypan, Bernard J. Hamrock,  
Herbert W. Scibbe, and William J. Anderson*

*Lewis Research Center  
Cleveland, Ohio 44135*





0133199

1. Report No. <b>NASA TN D-6607</b>		2. Government Accession No.		3. Recipient's Catalog No.	
4. Title and Subtitle <b>PREDICTED CHARACTERISTICS OF AN OPTIMIZED SERIES-HYBRID CONICAL HYDROSTATIC BALL BEARING</b>				5. Report Date <b>December 1971</b>	
				6. Performing Organization Code	
7. Author(s) <b>Lester J. Nypan, Bernard J. Hamrock, Herbert W. Scibbe, and William J. Anderson</b>				8. Performing Organization Report No. <b>E-6507</b>	
9. Performing Organization Name and Address <b>Lewis Research Center National Aeronautics and Space Administration Cleveland, Ohio 44135</b>				10. Work Unit No. <b>132-15</b>	
				11. Contract or Grant No.	
12. Sponsoring Agency Name and Address <b>National Aeronautics and Space Administration Washington, D. C. 20546</b>				13. Type of Report and Period Covered <b>Technical Note</b>	
				14. Sponsoring Agency Code	
15. Supplementary Notes					
16. Abstract  Optimized series-hybrid fluid-film ball bearings are described and operating characteristics are calculated and discussed. It is predicted that a series-hybrid bearing may be constructed which will reduce ball-bearing speed by 30 percent thereby increasing bearing fatigue life by factors of up to 5.9. Flow rates required are less than 9 kilograms per minute (20 lb/min).					
17. Key Words (Suggested by Author(s))  <b>Bearing Ball bearing Conical hydrostatic bearing</b>				18. Distribution Statement  <b>Unclassified - unlimited</b>	
19. Security Classif. (of this report) <b>Unclassified</b>		20. Security Classif. (of this page) <b>Unclassified</b>		21. No. of Pages <b>28</b>	
				22. Price* <b>\$3.00</b>	

# PREDICTED CHARACTERISTICS OF AN OPTIMIZED SERIES-HYBRID CONICAL HYDROSTATIC BALL BEARING

by Lester J. Nypan\*, Bernard J. Hamrock, Herbert W. Scibbe,  
and William J. Anderson  
Lewis Research Center

## SUMMARY

A series-hybrid bearing assembly consisting of a conical hydrostatic fluid-film bearing and a ball bearing is described. Computer studies are used to predict friction and life characteristics of 150-millimeter ball bearings. Conical hydrostatic fluid-film bearings are designed for minimum friction and maximum speed reduction of the ball-bearing component of the series-hybrid bearing. At a thrust load of 17 800 newtons (4000 lb) and speeds corresponding to DN (bearing bore in millimeters times shaft speed in rpm) values of 3 and 4 million, ball-bearing speed may be reduced by 30 percent. This speed reduction corresponds to ball-bearing fatigue life improvement factors of 3.4 at 3 million DN and 5.9 at 4 million DN. A flow rate of 8.25 kilograms per minute (18.2 lb/min) is required to maintain a fluid-film thickness of 0.025 millimeter (0.001 in.) in the hydrostatic bearing.

## INTRODUCTION

Increases power requirements for future gas turbine engines will result in the need for larger shaft diameters and higher mainshaft bearing speeds. Bearings in current production aircraft turbine engines operate in the range from 1.5 to 2 million DN (bearing bore in millimeters times shaft speed in rpm). Projected bearing DN values for aircraft turbine engines in the 1980's may be as high as 3 million (refs. 1 and 2).

At high speed the balls in a bearing orbit rapidly and cause high centrifugal loads at the outer race-ball contacts. These centrifugal loads, which increase Hertz stresses in a bearing above the level resulting from applied loads, can appreciably reduce bearing fatigue life. In order to achieve an ultimate DN capability of 3 to 4 million with an

---

\*Professor of Engineering, San Fernando State College, Northridge, California;  
NASA Summer Faculty Fellow in 1971.

acceptable fatigue life, several approaches are being taken to solve the high-speed bearing problem.

One approach for reducing stresses in high-speed bearings is through the use of low mass balls. Up to 50 percent weight reduction from that of a solid ball can be realized by fabricating a thin wall, spherically hollow ball or by drilling a concentric hole through the ball. The feasibility of both ball mass reducing methods has been demonstrated in full-scale bearings (refs. 3 and 4) with limited success.

A second technique that can be used to improve bearing life involves coupling a fluid-film bearing with a ball bearing. One approach couples the fluid-film and ball bearings in parallel so they share the thrust load. This concept was discussed as the hybrid boost bearing (ref. 5).

A third method for improving fatigue life is to reduce the rotational speed of the ball bearing by coupling it in series with the fluid-film bearing. In this arrangement, called the series-hybrid bearing, each bearing carries the full thrust load at part speed. Figure 1 illustrates this concept. The inner member of the fluid-film bearing rotates with the shaft at full shaft speed. The mating fluid-film bearing intermediate member rotates with the ball-bearing inner race at some fraction of the shaft speed. The outer race of the ball bearing is mounted in a stationary housing. Oil to pressurize the fluid-film bearing and to lubricate and cool the ball bearing may be obtained by centrifugal action through the shaft at the high speeds envisioned. An experimental study (ref. 6) was conducted with a combination self-acting journal and hydrostatic thrust fluid-film bearing coupled to a 75-millimeter-bore ball bearing. The lowest speed ratio (ball-bearing inner-race speed to shaft speed) obtained in the study of reference 6 was 0.67, which corresponded to a reduction in ball-bearing DN of one-third.

The objectives of this investigation are (1) to predict the operating characteristics of an optimally configured series-hybrid bearing at specific operating conditions, and (2) to determine whether the ball-bearing life would be sufficiently improved to warrant fabrication and experimental operation at thrust loads to 17 800 newtons (4000 lb) and DN values to 4 million.

The bearing system was optimized by (1) specifying ball diameter and complement for maximum life and speed reduction of a 150-millimeter ball bearing, and (2) specifying a conical hydrostatic fluid-film bearing configuration and dimensions to maximize speed reduction of the ball bearing.

## ANALYSIS

A characteristic of the operation of a series-hybrid fluid-film ball bearing system is that the torque causing rotation of the ball bearing is the friction torque transmitted

through the fluid-film bearing. As each component rotates under the action of the same torque, the speed of each bearing depends on the torque-speed relation of that component. Success of the series-hybrid bearing concept in reducing the speed of the ball-bearing component depends on the fluid-film bearing operating at an appreciable fraction of shaft speed.

To produce a long life series-hybrid bearing, factors that affect the life of the ball-bearing component must be considered. Ball-bearing friction torque is also of importance as the friction torque will determine the speed reduction that may be obtained from the fluid-film bearing.

## Ball-Bearing Characteristics

A computer program based on reference 7 was used to study the life and torque characteristics of a 150-millimeter angular contact ball bearing which was the rolling-element portion of the series-hybrid bearing.

Three studies were undertaken. The first study varied the number and diameter of balls. In this study, the number of balls was the largest complement that could be fitted into the bearing while still maintaining a minimum cage web thickness between ball pockets of 2.54 millimeters (0.100 in.) at the pitch diameter. Bearing running conditions investigated were speed parameter values of 3 and 4 million DN and thrust loads of 4450 newtons (1000 lb), as representative of a cruise condition of aircraft turbine engine operation, and 17 800 newtons (4000 lb), as representative of a maximum load or takeoff condition of operation.

Figure 2 shows the 10-percent ( $L_{10}$ ) fatigue life variation with ball diameter, using the maximum ball complement for each value of ball diameter. Maximum  $L_{10}$  life is obtained with the largest ball diameter. Figure 3 shows  $L_{10}$  life as a function of  $Zd^2$ , where  $Zd^2$  is proportional to the bearing (static) load capacity. (Symbols are defined in appendix A.) Life increases with  $Zd^2$ , though at high thrust load values, the slope of the curves decreases with  $Zd^2$  indicating smaller increases in life with an increase in  $Zd^2$ . Figure 4 shows bearing friction torque variation with ball diameter. Friction torque is not strongly affected by ball diameter, but is strongly influenced by load and speed. Torque decreases slightly with the number of balls at the high load condition, but increases slightly with number of balls at the low load condition. This may be due to the relative magnitude of the load and centrifugal force generated per ball at these large DN values.

In a second study, the maximum ball size was limited to less than 60 percent of the radial cross section (o.d. - i.d.)/2, to ensure adequate race stiffness and strength. In this study, the number of 22.2-millimeter- (0.8750-in. -) diameter balls was varied from

16 to 23, maintaining the same pitch diameter. The same speeds and loads were investigated. Figures 5 and 6 show bearing  $L_{10}$  life and friction torque variation with number of balls. The largest complement of balls yield the longest life. Figure 6 shows friction torque is slightly higher for the largest complement of balls. This relation will favor a greater speed share for the fluid-film bearing. Ball complement has a minor effect on friction torque, but torque is much more strongly affected by both bearing speed and load. To provide a cage web between ball pockets of 2.54 millimeters (0.100 in.) at the pitch diameter, the number of balls was restricted to 22.

The third computer study investigated bearing friction torque and fatigue life variation with speed and load for the 150-millimeter ball bearing incorporating 22 22.2-millimeter- (0.8750-in.-) diameter balls. Figure 7 shows ball bearing friction torque plotted as a function of speed for thrust loads of 4450 and 17 800 newtons (1000 and 4000 lb). Figure 8 shows bearing fatigue life in hours as a function of DN for thrust loads of 4450 to 17 800 newtons (1000 to 4000 lb).

Ball-bearing friction torque values are of considerable interest as they will strongly influence the success of the hybrid bearing concept in reducing ball-bearing speed. To evaluate the accuracy of torque predictions, the computer program was used to calculate torque values for bearings experimentally evaluated by Barwell and Hughes (ref. 8). These bearings were 127-millimeter bore, had 19 12.7-millimeter- (0.5000-in.-) diameter balls, and were oil jet lubricated. The bearings were operated at thrust loads from 2225 to 17 800 newtons (500 to 4000 lb) and a constant radial load of 2670 newtons (600 lb), at shaft speeds up to 11 000 rpm (DN value of 1.4 million). Comparison of measured and computed friction torque for these bearings indicated that the computer program (ref. 7) predicts values appreciably different from measured values. The largest differences were, however, less than an order of magnitude. Experimental data of Winn and Badgley (ref. 9) on the friction torque of 120-millimeter ball bearings, when compared to computed torque values, are also within an order of magnitude variation when differences in oil flow, viscosity, and bearing size are taken into account (appendix B).

## Fluid-Film Bearing Characteristics

A fluid-film bearing having a low torque rotational speed characteristic is required to obtain a large fluid-film speed share.

While a thrust load is the primary load in this application, the bearing must also have some radial load capacity. To avoid the complexity and reduce the friction of separate thrust and journal bearings, a conical hydrostatic bearing was selected as the fluid-film bearing component of the series-hybrid bearing system. A schematic of a conical hydrostatic bearing, indicating the location of the bearing land and pocket radii,

is shown in figure 9. The conical hydrostatic bearing will provide both thrust and radial load capacity. It can also be a useful component in an experimental apparatus as the fluid-film thickness can be simply controlled by adjusting the flow rate to the bearing.

Minimum friction conical hydrostatic bearings have been the subject of a recent study (ref. 10). This has resulted in the following expression for friction torque within the turbulent regime:

$$M_f = \frac{\pi \mu \omega_f R_1^4}{2h_L \sin \theta} \left[ X_4^4 - X_3^4 + X_2^4 - 1 + 0.0261 \left( \frac{\rho R_1 \omega_f h_p}{\mu} \right)^{0.75} f_r \frac{h_L}{h_p} (X_3^{4.75} - X_2^{4.75}) \right] \quad (1)$$

Preliminary calculations indicate that a hydrostatic bearing with a speed of 1700 rpm and using a Type II ester fluid at 366 K (200° F) will be operating within the turbulent regime ( $Re > 1000$ ). The hydrostatic bearing dimensions selected are compatible with the 150-millimeter ball bearing.

Reference 10 describes methods for the selection of bearing geometry to minimize friction torque. These methods are applied here to specify a minimum friction conical hydrostatic bearing to function as the fluid-film part of the series-hybrid bearing system operating at a shaft speed equivalent to a DN of 3 million (for a ball bearing) while supporting a 17 800-newton (4000-lb) thrust load. Operating characteristics of the bearing at a 4450-newton (1000-lb) thrust load and at bearing DN values of 3 and 4 million are also considered.

Oil may be fed to the bearing from the shaft centerline and pressure developed by centrifugal action. Centrifugal pressure available is

$$p = \frac{\rho \omega_s^2 R^2}{2} \quad (2)$$

From preliminary layouts, it appears that the innermost fluid-film bearing radius that will permit the largest shaft possible through the bearing, and still mate with the 150-millimeter ball bearing will be  $R_1 = 71.4$  millimeters (2.81 in.). If a Type II ester fluid is used, the density  $\rho$  will be  $9.4 \times 10^2$  kilograms per cubic meter ( $0.035 \text{ lb/in.}^3$ ) at 366 K (200° F). A centrifugal pressure of  $10.6 \times 10^6$  newtons per square meter (1530 psi) will then be available at a speed of 20 000 rpm (DN = 3 million). This is sufficient to support loads of 17 800 newtons (4000 lb) and provide compensation for misalignment and varying loads.

High thrust load condition (17 800 N or 4000 lb). - The dimensionless thrust parameter to be used in selecting a minimum friction bearing, from reference 10, is

$$\bar{F} = \frac{2F}{\pi p R_1^2} \quad (3)$$

Preliminary calculations have suggested a value of  $p = 4.44 \times 10^6$  newtons per square meter (645 psi) be used in equation (3). This allows a larger fraction of the available pressure for compensation than is suggested by Ling (ref. 11) for maximum stiffness. Stiffness will increase if load rises above the 17 800 newtons (4000 lb) considered. This gives a thrust parameter  $\bar{F}$  of 0.5. The friction torque  $M_f$  and bearing dimensions for a minimum friction conical hydrostatic bearing are determined from reference 10 as functions of the dimensionless flow parameter

$$\bar{Q} = \frac{6\mu Q}{\pi p h_L^3 \sin \theta} \quad (4)$$

Table I shows the predicted friction torque  $M_f$  as a function of flow parameter  $\bar{Q}$  for combinations of minimum fluid-film thickness  $h_L$  and fluid-film bearing speeds  $N_f$ . Minimum fluid-film thicknesses selected for consideration were  $h_L = 0.051, 0.025,$  and  $0.012$  millimeter (0.002, 0.001, and 0.0005 in.). Fluid-film bearing speeds  $N_f$  were calculated from  $\omega_f$  indicated in the hydrostatic pocket friction parameter

$$C_2 = 0.0261 \left( \frac{\rho R_1 \omega_f h_p}{\mu} \right)^{0.75} f_r \frac{h_L}{h_p} \quad (5)$$

with values of  $C_2 = 0.8, 0.4,$  and  $0.2$  for pocket depth  $h_p = 6.35$  and  $3.18$  millimeters (0.25 and 0.125 in.). These large pocket depths were selected to reduce pocket friction torque. Table I gives values of  $\bar{M}_f$  associated with  $\bar{Q}$  values for  $\bar{F} = 0.5$ ,  $C_2$  values specified previously, and the speed listed. Dimensionless  $\bar{Q}$  is converted to dimensional flow rate  $Q$  using equation (4), and using the density of  $\rho = 9.4 \times 10^2$  kilograms per cubic meter (0.034 lb/in.<sup>3</sup>), is given in kilograms per minute (lb/min) for comparison with flow rates commonly encountered in bearing lubrication and cooling. Dimensionless friction torque  $\bar{M}$  is converted to dimensional friction torque  $M$  from

$$\bar{M} = \frac{2M_f h_L \sin \theta}{\pi \mu \omega_f R_1^4} \quad (6)$$

The half cone angle  $\theta$  was taken to be  $45^\circ$ . The viscosity  $\mu$  of the Type II ester at



366 K (200° F) is  $5.5 \times 10^{-3}$  newton per second per square meter ( $0.8 \times 10^{-6}$  (lb)(sec)/in.<sup>2</sup>). It may be noted in table I that changing  $h_L$  from 0.051 to 0.025 millimeter (0.002 to 0.001 in.) reduces the flow  $Q$  by seven-eighths and doubles the friction torque  $M_f$ . Values tabulated for the 0.051-millimeter (0.002-in.) fluid-film thickness indicate that flow requirements are so large as to make bearing operation at this film thickness impractical.

Values of friction torque from table I are plotted as functions of fluid-film bearing speed in figure 10. Also shown in figure 10 is the predicted ball-bearing friction torque at speeds compatible with the fluid-film bearing speed and shaft speed for DN values of 3 and 4 million. Possible operating points for the hybrid bearing system are the intersections of the curves.

Figure 10 and table I indicate that the 0.025-millimeter (0.001-in.) fluid-film thickness operating conditions could have a substantial fluid-film speed share at flow rates comparable to those presently used to lubricate and cool aircraft gas turbine engine bearings. Figures 10(a) and (c) show results for hydrostatic pocket depths of 6.35 and 3.18 millimeters (0.250 and 0.125 in.), respectively, and the 0.025-millimeter (0.001-in.) fluid-film thickness. Figures 10(b) and (d) show results for hydrostatic pocket depths of 6.35 and 3.18 millimeters (0.250 and 0.125 in.), respectively, and a 0.012-millimeter (0.0005-in.) fluid-film thickness.

Table II gives optimum bearing dimensions for values of flow parameter  $\bar{Q}$ . Radii  $R_1$  and  $R_2$  are those of the inner land, while  $R_3$  and  $R_4$  are those of the outer land (fig. 9). As was noted in reference 10, bearing dimensions are insensitive to changes in the hydrostatic pocket friction parameter  $C_2$  so that only one set of bearing dimensions is obtained. For a given thrust load then, bearing dimensions depend only on flow parameter  $\bar{Q}$  and the single table of dimensions is sufficient to specify minimum friction bearings for the assumed design conditions. Figure 11 shows the relative proportions of these bearings. These range from the configuration of  $\bar{Q} = 20$  where the hydrostatic pocket is shrunk into what is practically a line fed hydrostatic pad to the configuration of  $\bar{Q} = 1000$  where the lands have diminished to less than 0.25 millimeter (0.01 in.).

Low thrust load condition. - The relation among flow, thrust load, and minimum fluid-film thickness may be obtained (ref. 10) from

$$Q = \frac{\pi p h_L^3 \sin \theta}{6\mu} \left( \frac{1}{\ln \frac{R_2}{R_1}} + \frac{1}{\ln \frac{R_4}{R_3}} \right) \quad (7)$$

and

$$F = \frac{\pi p}{2} (R_4^2 + R_3^2 - R_2^2 - R_1^2) \quad (8)$$

or

$$Q = \frac{F h_L^3 \sin \theta}{3\mu (R_4^2 + R_3^2 - R_2^2 - R_1^2)} \left( \frac{1}{\ln \frac{R_2}{R_1}} + \frac{1}{\ln \frac{R_4}{R_3}} \right) \quad (9)$$

For a given bearing and lubricant  $Q = k F h_L^3$  where  $k$  is a constant for the bearing and lubricant. At the 17 800-newton (4000-lb) thrust load and design flow rate, the film thickness and friction torque have been determined. At the 4450-newton (1000-lb) thrust load and the same design flow rate, the minimum film thickness is then 1.59 times the fluid-film thickness for the 17 800-newton (4000-lb) thrust load. Friction torque may then be calculated from equation (1). Figure 12 shows the torque-speed characteristics expected at the 4450-newton (1000-lb) thrust load condition for 3.18-millimeter (0.125-in.) pocket bearings.

### Predicted Speed Share and Life Improvement

After determining the friction torque-speed characteristics for the ball bearing and the fluid-film bearing, the speed sharing performance of the series-hybrid bearing may be predicted. From this speed sharing, the life improvement of the series-hybrid bearing over the unassisted ball bearing is determined.

The sum of the speeds of the fluid-film bearing and the ball bearing will be equal to the shaft speed, that is,  $\omega_s = \omega_f + \omega_b$ . The torque-speed characteristics of the two bearing components of the series-hybrid bearing may be conveniently compared by plotting fluid-film bearing torque  $M_f$  as a function of fluid-film bearing speed  $\omega_f$  and ball-bearing torque  $M_b$  as a function of ball-bearing speed  $\omega_b = \omega_s - \omega_f$  on the same axes. The operating speed of the fluid-film bearing is then readily determined as the speed consistent with the common torque  $M_f = M_b$ , operating to drive the bearings at the speeds  $\omega_f$  and  $\omega_b = \omega_s - \omega_f$ .

Figure 10 shows torque-speed curves of five possible fluid film bearings operating at a 17 800-newton (4000-lb) thrust load with fluid film thicknesses 0.025 and 0.012 millimeter (0.001 and 0.0005 in.). Friction torque curves for the 150-millimeter ball bearing in a series-hybrid bearing operating at shaft speeds of 20 000 and 26 667 rpm (DN = 3 and 4 million for the 150-mm bearing) are also shown. Points of intersection

indicate operating conditions of equal torque and compatible bearing speeds.

Figure 10 indicates that substantial speed ratios (speed ratio = ball bearing speed/shaft speed) may be obtained. Table III shows, for example, at a  $\bar{Q}$  value of 30 and a 3.18-millimeter (0.125-in.) pocket depth, a bearing operating at a fluid-film thickness of 0.025 millimeter (0.001 in.) will require a flow rate of 8.26 kilograms per minute (18.2 lb/min). These operating conditions would provide speed ratios of 0.68 at the 20 000-rpm shaft speed and 0.70 at the 26 667-rpm shaft speed for a 17 800-newton (4000-lb) thrust load. Table III also gives values of predicted speed ratios for bearings having  $\bar{Q}$  values of 20, 70, and 100 at the two speeds for 3.18-millimeter- (0.125-in.-) deep pockets. Examination of predicted speeds for bearings with a 6.36-millimeter (0.250-in.) pocket depth indicated an increase of less than 1 percent in speed ratio at flow rates less than 19.3 kilograms per minute (42.6 lb/min). Figure 12 shows torque-speed curves similar to those of figure 10 for the 4450-newton (1000-lb) thrust load condition. Predicted speed ratios for this condition are also given in table III.

The 8.26-kilogram-per-minute (18.2-lb/min) flow rate required is nearly the same as the 20 pounds per minute mentioned by Brown (ref. 2) used for cooling and lubrication of advanced engine mainshaft bearings.

The potential increase in ball bearing fatigue life due to a reduction in the effective DN value can be seen from figure 8. With the 150-millimeter-bore ball bearing operating at a DN of 3 million and 17 800-newton (4000-lb) thrust load, its expected  $L_{10}$  fatigue life is 520 hours. If the same bearing is operated in a series-hybrid arrangement with a speed ratio of 0.7, its effective DN is 2.1 million and its  $L_{10}$  fatigue life is 1750 hours. The life improvement factor is  $1750/520 = 3.4$ . With the 17 800-newton (4000-lb) thrust load, at a DN of 4 million and speed ratio of 0.7, the  $L_{10}$  life of 120 hours would improve to 710 hours at an effective DN of 2.8 million for a life improvement factor of 5.9.

In the 4450-newton (1000-lb) thrust load cases, the speed ratio of 0.7 again provides effective DN values of 2.1 and 2.8 million for shaft speeds corresponding to a DN of 3 and 4 million with life improvement ratios of 3.9 and 7.1.

## CONCLUSIONS

A series-hybrid fluid-film ball bearing may be constructed to reduce ball bearing speed by 30 percent. Relatively moderate flow rates are required for its operation. At a 17 800-newton (4000-lb) thrust load and shaft speeds corresponding to speed parameter DN values of 3 and 4 million for a 150-millimeter ball bearing, a flow of 8.26 kilograms

per minute (18.2 lb/min) is required to maintain a fluid-film thickness of 0.025 millimeter (0.001 in.) for the optimum bearing dimensions. The resulting life improvement factors are 3.4 and 5.9 for DN values of 3 and 4 million, respectively.

Lewis Research Center,  
National Aeronautics and Space Administration,  
Cleveland, Ohio, September 24, 1971,  
132-15.

## APPENDIX A

### SYMBOLS

$C_2$	dimensionless turbulent friction coefficient $0.0261 f_r (\rho R_1 \omega_f h_p / \mu)^{0.75} (h_L / h_p)$
$D$	ball-bearing bore diameter, mm (in.)
$d$	ball diameter, mm (in.)
$F$	thrust load, N (lb)
$\bar{F}$	dimensionless thrust load parameter, $2F / \pi p R_1^2$
$f_r$	fraction of area between $R_2$ and $R_3$ occupied by hydrostatic pockets (usually may be approximated by 1)
$h$	fluid-film thickness, mm (in.)
$M$	friction torque, m-N (in.-lb)
$\bar{M}$	dimensionless friction torque, m-N (in.-lb)
$M_b$	ball-bearing torque, m-N (in.-lb)
$M_f$	fluid-film bearing torque, m-N (in.-lb)
$\bar{M}_f$	dimensionless fluid-film bearing torque, $2M_f h_L \sin \theta / \pi \mu \omega_f$
$m$	oil mass flow rate, kg/min (lb/min)
$N$	ball-bearing speed, rpm
$N_f$	fluid-film bearing speed, rpm
$N_s$	shaft speed, rpm
$p$	pressure, N/m <sup>2</sup> (lb/in. <sup>2</sup> )
$Q$	fluid flow, m <sup>3</sup> /sec (in. <sup>3</sup> /sec)
$\bar{Q}$	dimensionless fluid-flow parameter, $6\mu Q / \pi h_L^3 p \sin \theta$
$q$	power loss rejected to the oil, W (hp)
$R$	typical radius on fluid-film bearing, mm (in.)
$R_1$	inner radius of inner land, mm (in.)
$R_2$	outer radius of inner land, mm (in.)
$R_3$	inner radius of outer land, mm (in.)
$R_4$	outer radius of outer land, mm (in.)
$Re$	Reynolds number, $\rho V h / \mu$

$V$	bearing surface speed, m/sec (in./sec)
$X_2$	$R_2/R_1$
$X_3$	$R_3/R_1$
$X_4$	$R_4/R_1$
$Z$	number of balls
$\theta$	half angle of conical hydrostatic bearing, deg
$\mu$	fluid dynamic viscosity, N-sec/m <sup>2</sup> (lb-sec/in. <sup>2</sup> )
$\rho$	fluid density, kg/m <sup>3</sup> (lb/in. <sup>3</sup> )
$\omega_b$	rotational speed of ball bearing, rad/sec
$\omega_f$	rotational speed of fluid-film bearing, rad/sec
$\omega_s$	rotational speed of shaft, $\omega_b + \omega_f$ , rad/sec

Subscripts:

$L$	land
$p$	pocket

## APPENDIX B

### CALCULATED AND MEASURED POWER LOSS FOR 120-MILLIMETER- BORE BALL BEARINGS

Winn and Badgley in reference 9 present measured and calculated values of power loss for a 120-millimeter-bore angular-contact ball bearing. In tables X, XI, and XII the power losses are given for an oil flow rate of  $0.63 \times 10^{-4}$  cubic meter per second (1 gpm) at temperatures of 311, 366, and 422 K ( $100^{\circ}$ ,  $200^{\circ}$ , and  $300^{\circ}$  F), respectively. Bearing thrust load ranged from 1113 to 12 640 newtons (250 to 2840 lb) at speeds from 4000 to 10 000 rpm (0.48 to 1.20 million DN). The calculated power loss was based on an empirical equation developed by Nemeth, Macks, and Anderson (ref. 12) which gives power loss rejected to the oil as

$$q = 3.19 \times 10^{-8} \text{ DN}^{1.5} F^{0.07} \mu^{0.25} m^{0.42} \quad (\text{B1})$$

The data of table XI (ref. 9) for the 366 K ( $200^{\circ}$  F) tests are most nearly comparable to the design condition of concern in this work. Reference 9 gives the effect of a  $1.26 \times 10^{-4}$ -cubic-meter-per-second (2-gpm) flow rate on the friction torques measured as increasing the power losses over those of the  $0.63 \times 10^{-4}$ -cubic-meter-per-second (1-gpm) flow rate by 30 and 50 percent, respectively, for the 8000- and 10 000-rpm bearing speeds.

Before equation (B1) can be used to determine power loss for the 150-millimeter ball bearing in the present study, a viscosity-diameter correction factor of 1.61 must be applied to account for the differences in oil viscosity and bearing size. When increases of 30- and 50-percent are also applied, as noted previously, to account for an oil flow rate of  $1.26 \times 10^{-4}$  cubic meter per second (2 gpm) corresponding to a 7.12-kilogram-per-minute (15.7-lb/min) flow rate in the hybrid bearing assembly, the factor becomes 2.1 and 2.4, respectively, for the 8000- and 10 000-rpm cases reported. When these factors are applied to the average of the power losses reported for these speeds, and the result converted to torque, the torque values are 3.34-meter-newtons (29.6 in.-lb) at 8000 rpm and 6.5 meter-newtons (57.5 in.-lb) at 10 000 rpm. In view of the difficulty in replicating all of the factors involved and the difficulty in predicting friction torques, these values seem to adequately check the predicted bearing torques of figure 7.

## REFERENCES

1. Coe, Harold H.; Scibbe, Herbert W.; and Parker, Richard J.: Performance of 75-Millimeter-Bore Bearings to 1.8 Million DN with Electron-Beam-Welded Hollow Balls. NASA TN D-5800, 1970.
2. Brown, Paul F.: Bearings and Dampers for Advanced Jet Engines. Paper 700318, SAE, Apr. 1970.
3. Coe, Harold H.; Parker, Richard J.; and Scibbe, Herbert W.: Evaluation of Electron-Beam Welded Hollow Balls for High-Speed Ball Bearings. J. Lubr. Tech., vol. 93, no. 1, Jan. 1971, pp. 47-59.
4. Coe, Harold H.; Scibbe, Herbert W.; and Anderson, William J.: Evaluation of Cylindrically Hollow (Drilled) Balls in Ball Bearings at DN Values to 2.1 Million. NASA TN D-7007, 1971.
5. Wilcock, Donald F.; and Winn, Leo W.: The Hybrid Boost Bearing - A Method of Obtaining Long Life in Rolling Contact Bearing Applications. J. Lubr. Tech., vol. 92, no. 3, July 1970, pp. 406-414.
6. Parker, Richard J.; Fleming, David P.; Anderson, William J.; and Coe, Harold H.: Experimental Evaluation of the Series-Hybrid Rolling-Element Bearing. NASA TN D-7011, 1970.
7. Althouse, R. C.; and Harris, T. A.: Analytical Evaluation of Performance of a 75-mm Bore Thrust, Angular Contact Ball Bearing. NASA CR 72692, 1970.
8. Barwell, F. T.; and Hughes, M. J.: Some Further Tests on High-Speed Ball-Bearings. Proc. Inst. Mech Eng., vol. 169, no. 36, 1955, pp. 699-706.
9. Winn, L. W.; and Badgley, R. H.: Development of Long Life Jet Engine Thrust Bearings. Rep. MTI-70TR44, Mechanical Technology, Inc. (NASA CR 72744), June 1970.
10. Nypan, Lester J.; Hamrock, Bernard J.; Scibbe, Herbert W.; and Anderson, William J.: Optimization of Conical Hydrostatic Bearing for Minimum Friction. NASA TN D-6371, 1971.
11. Ling, Marvin T. S.: On the Optimization of the Stiffness of Externally Pressurized Bearings. J. Basic Eng., vol. 84, no. 1, Mar. 1962, pp. 119-122.
12. Nemeth, Zolton N.; Macks, E. Fred; and Anderson, William J.: Investigation of 75-Millimeter-Bore Deep-Grooved Ball Bearings Under Radial Load at High Speeds. II - Oil Inlet Temperature, Viscosity, and Generalized Cooling Correlation. NACA TN 3003, 1953.



TABLE I. - FLOW AND FRICTION TORQUE FOR THREE FLUID-FILM THICKNESSES

(a) Pocket depth  $h_p = 6.35$  millimeters (0.250 in.)

Dimensionless flow rate, $\bar{Q}$	Fluid flow, $Q$		Dimensionless friction torque, $\bar{M}$	Fluid-film bearing torque, $M_f$		Dimensionless friction torque, $\bar{M}$	Fluid-film bearing torque, $M_f$	
	$\frac{\text{kg}}{\text{min}}$	$\frac{\text{lb}}{\text{min}}$		m-N	in. -lb		m-N	in. -lb
				$h_L = 0.051 \text{ mm (0.002 in.)}; C_2 = 0.8; N_f = 5869 \text{ rpm}$		$h_L = 0.051 \text{ mm (0.002 in.)}; C_2 = 0.4; N_f = 2329 \text{ rpm}$		
20	43.6	96.2	1.239	6.03	53.3	1.235	2.390	21.10
30	66.2	146.0	.989	4.82	42.6	.879	1.699	15.01
70	154.2	340.0	.732	3.56	31.5	.520	1.003	8.88
100	220.4	486.0	.679	3.30	29.2	.445	.859	7.60
1000	2205.8	4863.0	.571	2.78	24.6	.296	.572	5.06

Dimensionless flow rate, $\bar{Q}$	Fluid flow, $Q$		Dimensionless friction torque, $\bar{M}$	Fluid-film bearing torque, $M_f$		Dimensionless friction torque, $\bar{M}$	Fluid-film bearing torque, $M_f$	
	$\frac{\text{kg}}{\text{min}}$	$\frac{\text{lb}}{\text{min}}$		m-N	in. -lb		m-N	in. -lb
				$h_L = 0.025 \text{ mm (0.001 in.)}; C_2 = 0.8; N_f = 18\ 633 \text{ rpm}$		$h_L = 0.025 \text{ mm (0.001 in.)}; C_2 = 0.4; N_f = 7394 \text{ rpm}$		
20	5.48	12.1	1.239	30.3	268	1.235	12.00	106.1
30	8.26	18.2	.989	24.2	214	.879	8.55	75.6
70	19.32	42.6	.732	18.0	159	.520	5.05	44.7
100	27.58	60.8	.679	16.6	147	.445	4.33	38.3
1000	275.78	608.0	.571	14.0	124	.296	2.88	25.5

Dimensionless flow rate, $\bar{Q}$	Fluid flow, $Q$		Dimensionless friction torque, $\bar{M}$	Fluid-film bearing torque, $M_f$		Dimensionless friction torque, $\bar{M}$	Fluid-film bearing torque, $M_f$	
	$\frac{\text{kg}}{\text{min}}$	$\frac{\text{lb}}{\text{min}}$		m-N	in. -lb		m-N	in. -lb
				$h_L = 0.012 \text{ mm (0.0005 in.)}; C_2 = 0.4; N_f = 18\ 633 \text{ rpm}$		$h_L = 0.012 \text{ mm (0.0005 in.)}; C_2 = 0.2; N_f = 7394 \text{ rpm}$		
20	0.69	1.52	1.235	60.6	536	1.232	23.95	212.0
30	1.03	2.28	.879	43.1	381	.824	16.02	141.8
70	2.41	5.32	.520	25.6	226	.413	8.04	71.1
100	3.45	7.60	.445	21.8	193	.328	6.38	56.4
1000	34.46	75.99	.296	14.5	128	.158	3.07	27.2

TABLE I. - Concluded. FLOW AND FRICTION TORQUE FOR THREE  
FLUID-FILM THICKNESSES

(b) Pocket depth  $h_p = 3.18$  millimeters (0.125 in.)

Dimen- sionless flow rate, $\bar{Q}$	Fluid flow, $Q$		Dimen- sionless friction torque, $\bar{M}$	Fluid-film bearing torque, $M_f$		Dimen- sionless friction torque, $\bar{M}$	Fluid-film bearing torque, $M_f$	
	$\frac{kg}{min}$	$\frac{lb}{min}$		m-N	in. -lb		m-N	in. -lb
			$h_L = 0.051 \text{ mm (0.002 in.)};$ $C_2 = 0.8; N_f = 5869 \text{ rpm}$		$h_L = 0.051 \text{ mm (0.002 in.)};$ $C_2 = 0.4; N_f = 2329 \text{ rpm}$			
20	43.6	96.2	1.239	4.77	42.2	1.235	1.887	16.70
30	66.2	146.0	.989	3.82	33.8	.879	1.347	11.91
70	154.2	340.0	.732	2.82	25.0	.520	.796	7.05
100	220.4	486.0	.679	2.62	23.2	.445	.682	6.03
1000	2205.8	4863.0	.571	2.21	19.5	.296	.453	4.01

Dimen- sionless flow rate, $\overline{Q}$	Fluid flow $Q$		Dimen- sionless friction torque, $\overline{M}$	Fluid-film bearing torque, $M_f$		Dimen- sionless friction torque, $\overline{M}$	Fluid-film bearing torque, $M_f$	
	$\frac{kg}{min}$	$\frac{lb}{min}$					m-N	in. -lb
			$h_L = 0.025 \text{ mm (0.001 in.)};$ $C_2 = 0.8; N_f = 14\,789 \text{ rpm}$			$h_L = 0.025 \text{ mm (0.001 in.)};$ $C_2 = 0.4; N_f = 5869 \text{ rpm}$		
20	5.48	12.1	1.239	2.41	213	1.235	9.53	84.4
30	8.26	18.2	.989	1.92	170	.879	6.78	60.0
70	19.32	42.6	.732	1.42	126	.520	4.02	35.5
100	27.58	60.8	.679	1.32	117	.445	3.43	30.4
1000	275.78	608.0	.571	1.11	98	.296	2.28	20.2

Dimen- sionless flow rate, $\overline{Q}$	Fluid flow, Q		Dimen- sionless friction torque, $\overline{M}$	Fluid-film bearing torque, $M_f$		Dimen- sionless friction torque, $\overline{M}$	Fluid-film bearing torque, $M_f$	
	$\frac{kg}{min}$	$\frac{lb}{min}$		m-N	in. -lb		m-N	in. -lb
				$h_L = 0.012 \text{ mm (0.0005 in.)};$ $C_2 = 0.4; N_f = 14\,789 \text{ rpm}$		$h_L = 0.012 \text{ mm (0.0005 in.)};$ $C_2 = 0.2; N_f = 5869 \text{ rpm}$		
20	0.69	1.52	1.235	48.2	426	1.232	18.87	167.0
30	1.03	2.28	.879	34.2	303	.824	12.72	112.6
70	2.41	5.32	.520	20.2	179	.413	6.38	56.4
100	3.45	7.60	.445	17.3	153	.328	5.07	44.8
1000	34.46	75.99	.296	11.5	102	.158	2.44	21.6

TABLE II. - OPTIMUM BEARING DIMENSIONS (FOR ALL VALUES OF

$$C_2 \text{ AND } \bar{F} = 0.5)$$

Dimensionless flow rate, $\bar{Q}$	Inner radius of inner land, $R_1$		Outer radius of inner land, $R_2$		Inner radius of outer land, $R_3$		Outer radius of outer land, $R_4$	
	mm	in.	mm	in.	mm	in.	mm	in.
20	71.42	2.812	78.87	3.105	78.99	3.110	87.38	3.440
30	↓	↓	76.50	3.012	79.43	3.127	84.79	3.338
70			73.63	2.899	79.70	3.138	81.92	3.225
100			73.00	2.874	79.78	3.141	81.28	3.200
1000	↓	↓	71.58	2.818	79.80	3.144	79.98	3.149

TABLE III. - PREDICTED SPEED RATIOS (BALL BEARING SPEED/SHAFT SPEED)

$$[\text{Pocket depth } h_p = 3.18 \text{ mm (0.125 in.)}]$$

(a) 17 800-Newton (4000-lb) thrust load

Dimen- sionless flow rate, $\bar{Q}$	Fluid flow, Q		Shaft speed, $N_s$ , rpm		Fluid flow, Q		Shaft speed, $N_s$ , rpm	
	$\frac{\text{kg}}{\text{min}}$	$\frac{\text{lb}}{\text{min}}$	20 000	26 667	$\frac{\text{kg}}{\text{min}}$	$\frac{\text{lb}}{\text{min}}$	20 000	26 667
			Speed ratio				Speed ratio	
	$h_L = 0.025 \text{ mm (0.001 in.)}$				$h_L = 0.012 \text{ mm (0.0005 in.)}$			
20	5.48	12.1	0.75	0.78	0.691	1.52	0.86	0.87
30	8.26	18.2	.68	.70	1.034	2.28	.80	.81
70	19.32	42.6	.59	.62	2.420	5.32	.67	.70
100	27.58	60.8	.57	.60	3.455	7.60	.63	.66

(b) 4450-Newton (1000-lb) thrust load

Dimen- sionless flow rate, $\bar{Q}$	Fluid flow, Q		Shaft speed, $N_s$ , rpm		Fluid flow, Q		Shaft speed, $N_s$ , rpm	
	$\frac{\text{kg}}{\text{min}}$	$\frac{\text{lb}}{\text{min}}$	20 000	26 667	$\frac{\text{kg}}{\text{min}}$	$\frac{\text{lb}}{\text{min}}$	20 000	26 667
			Speed ratio				Speed ratio	
	$h_L = 0.04 \text{ mm (0.00159 in.)}$				$h_L = 0.02 \text{ mm (0.00079 in.)}$			
20	5.48	12.1	0.72	0.71	0.691	1.52	0.83	0.83
30	8.26	18.2	.61	.67	1.034	2.28	.78	.78
70	19.32	42.6	.60	.60	2.420	5.32	.67	.67
100	27.58	60.8	.57	.60	3.455	7.60	.64	.64

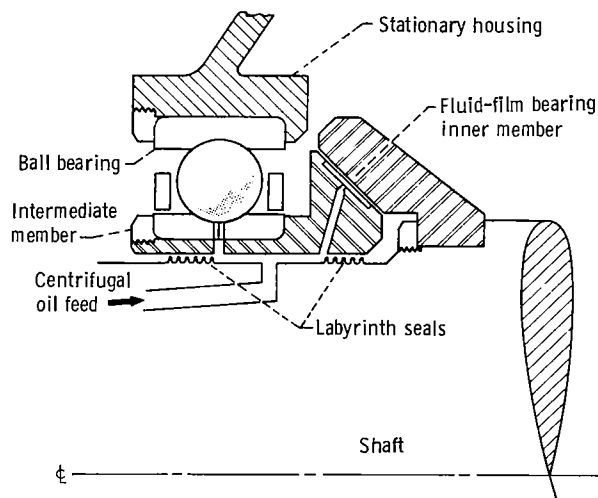


Figure 1. - Schematic diagram of a typical series-hybrid fluid-film, rolling element bearing.

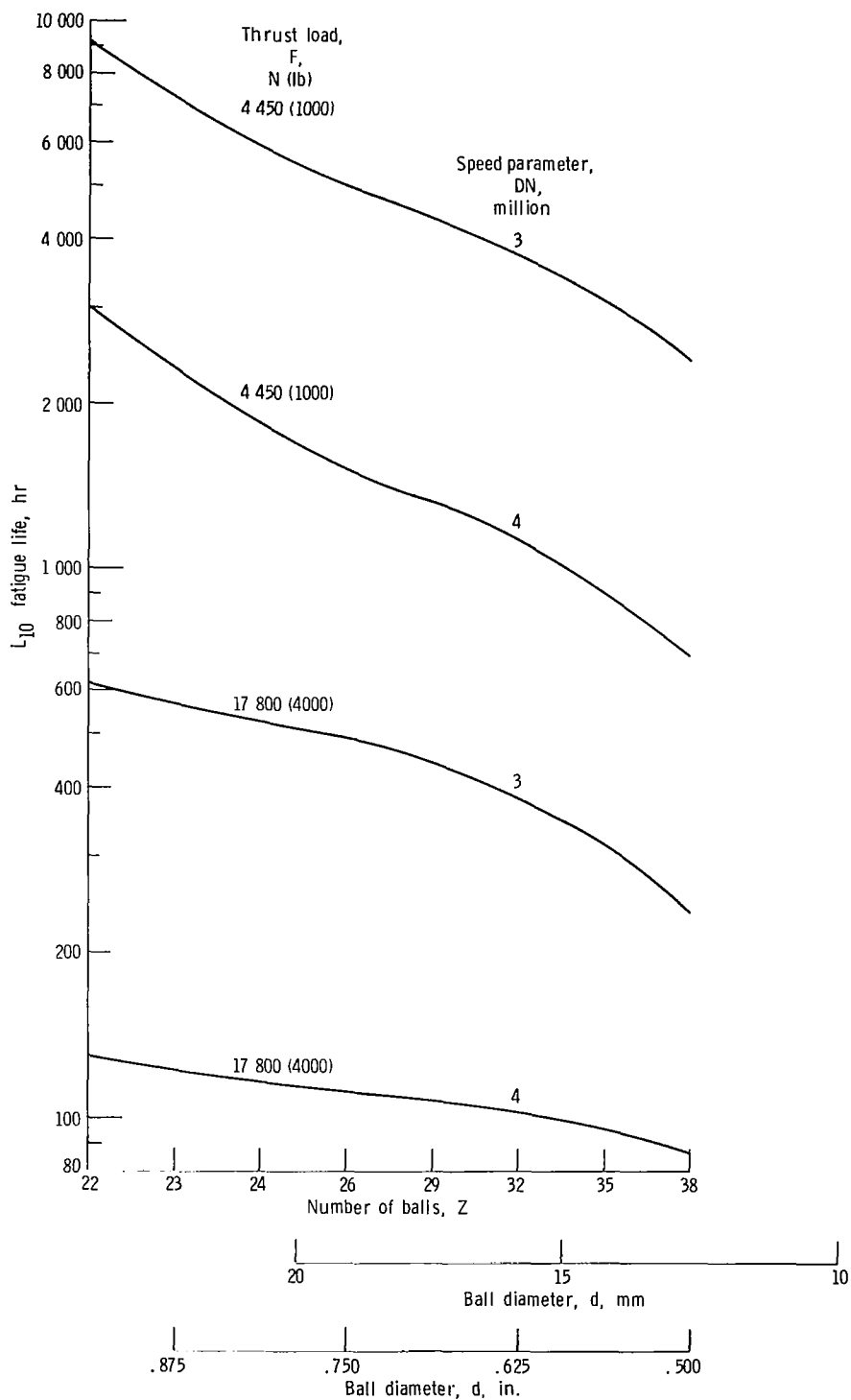


Figure 2. -  $L_{10}$  fatigue life as a function of ball diameter (maximum ball complement), for 150-millimeter-bore ball bearing. Pitch diameter, 188 millimeters (7.358 in.).

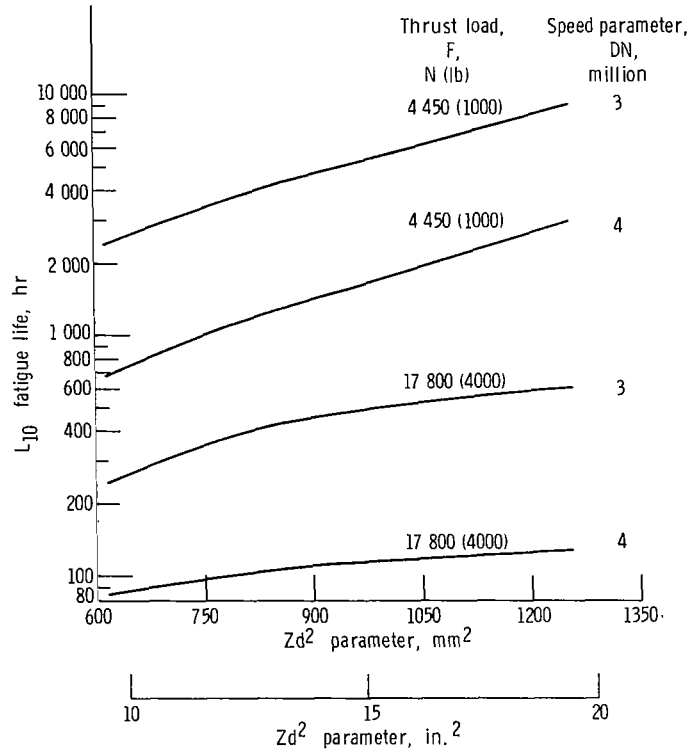


Figure 3. -  $L_{10}$  fatigue life as a function of  $Zd^2$  (maximum ball complement) for 150-millimeter-bore ball bearing.

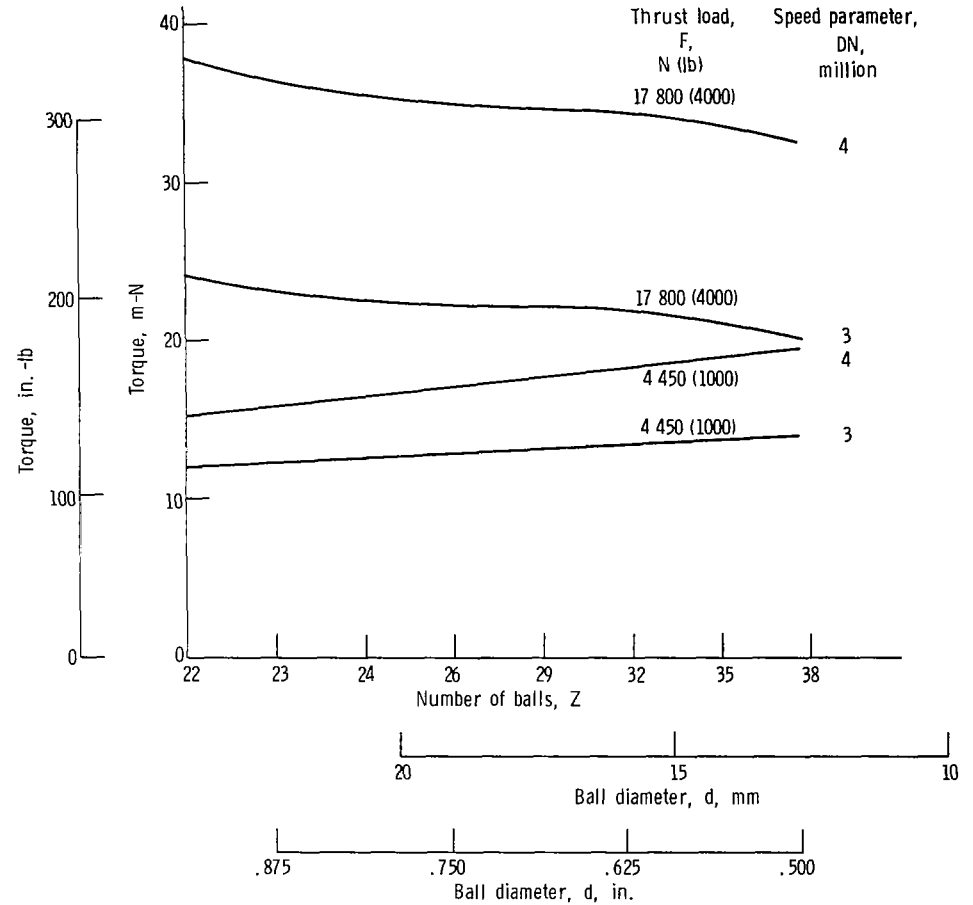


Figure 4. - Friction torque as a function of ball diameter (maximum ball complement) for 150-millimeter-bore ball bearing. Pitch diameter, 188 millimeters (7.358 in.).

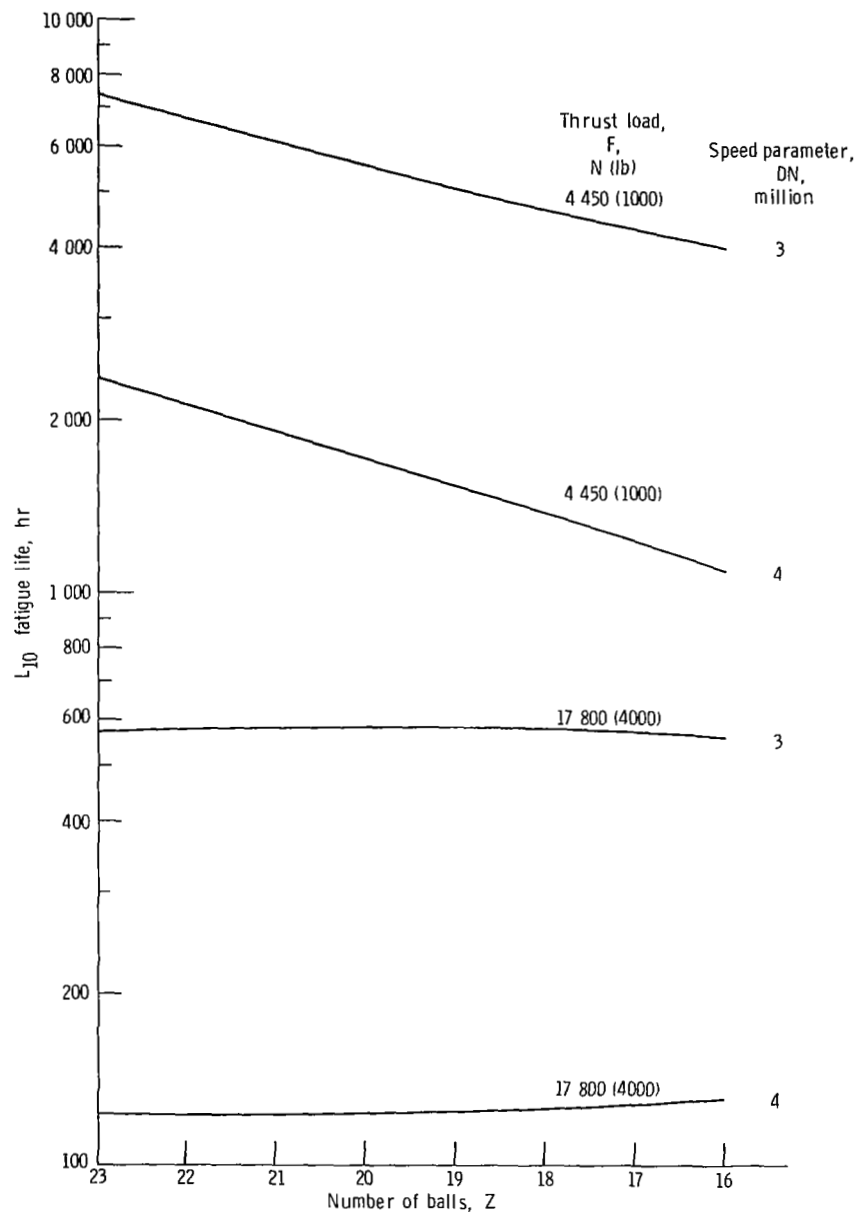


Figure 5. -  $L_{10}$  fatigue life as a function of ball complement for 150-millimeter-bore ball bearing. Ball diameter, 22.2 millimeters (0.875 in.); pitch diameter, 188 millimeters (7.358 in.).

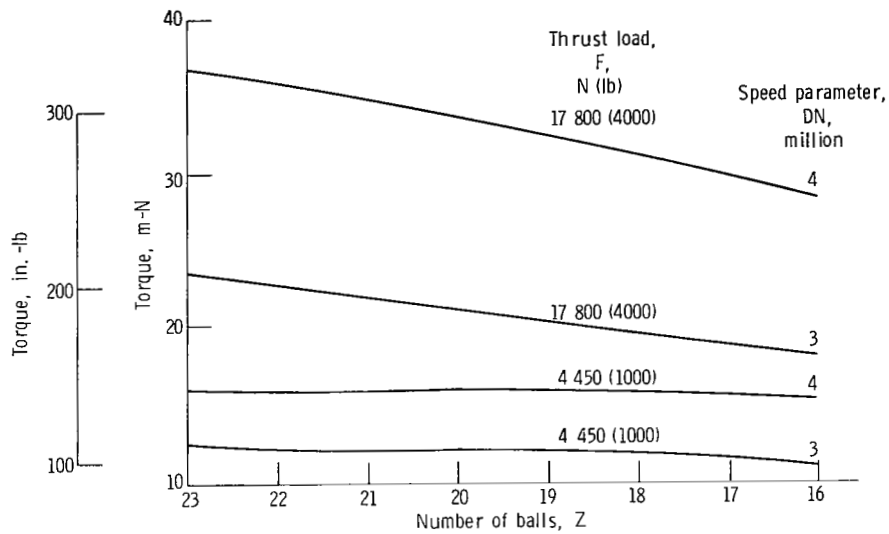


Figure 6. - Friction torque as a function of ball complement for 150-millimeter-bore ball bearing. Ball diameter, 22.2 millimeters (0.875 in.); pitch diameter, 188 millimeters (7.358 in.).

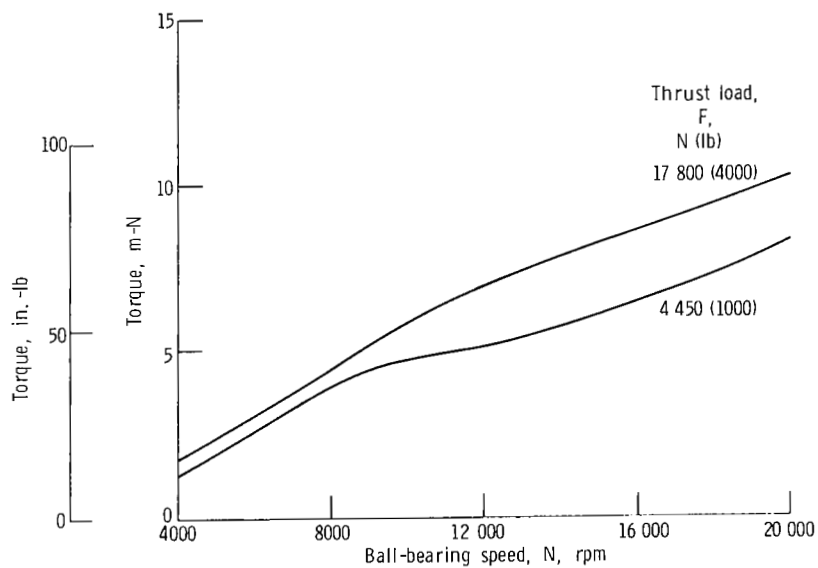


Figure 7. - Computed torque-speed relation for a 150-millimeter-bore bearing. Ball diameter, 22.2 millimeters (0.875 in.); pitch diameter, 188 millimeters (7.358 in.).



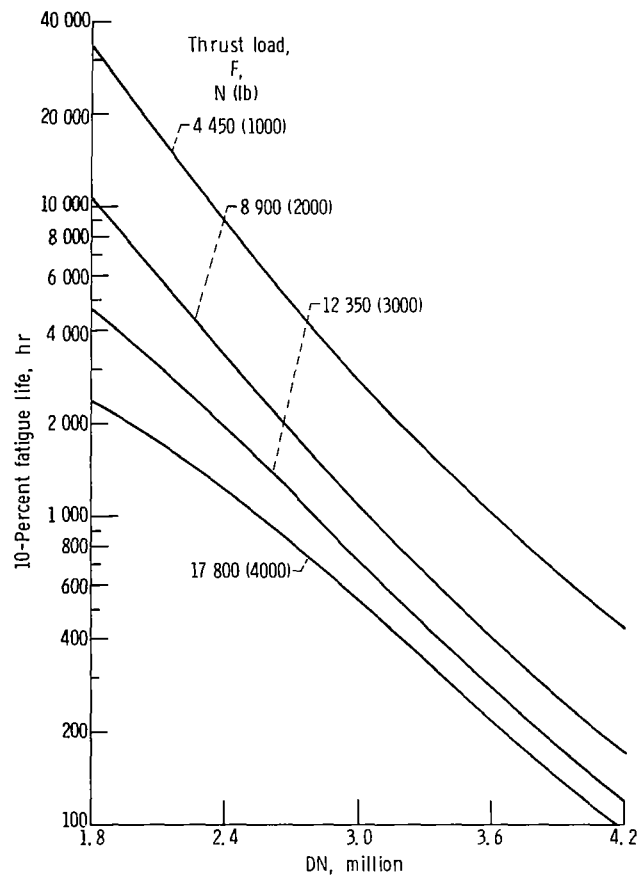
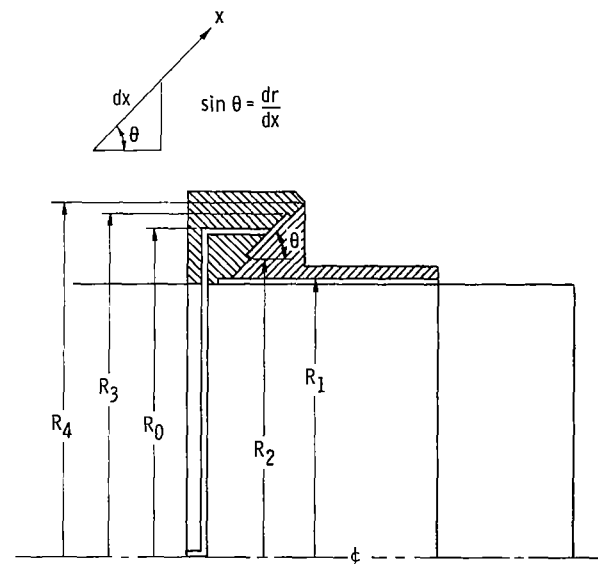
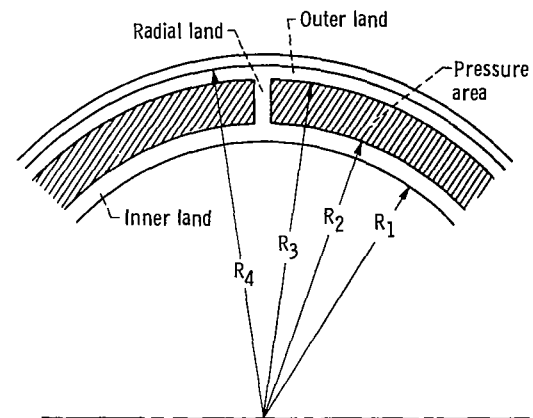


Figure 8. - Theoretical fatigue life of thrust-loaded 150-millimeter-bore ball bearing, based on analysis of reference 7. (Data from ref. 6.)



(a) Section view.



(b) Front view.

Figure 9. - Schematic diagrams of conical hydrostatic bearing design.

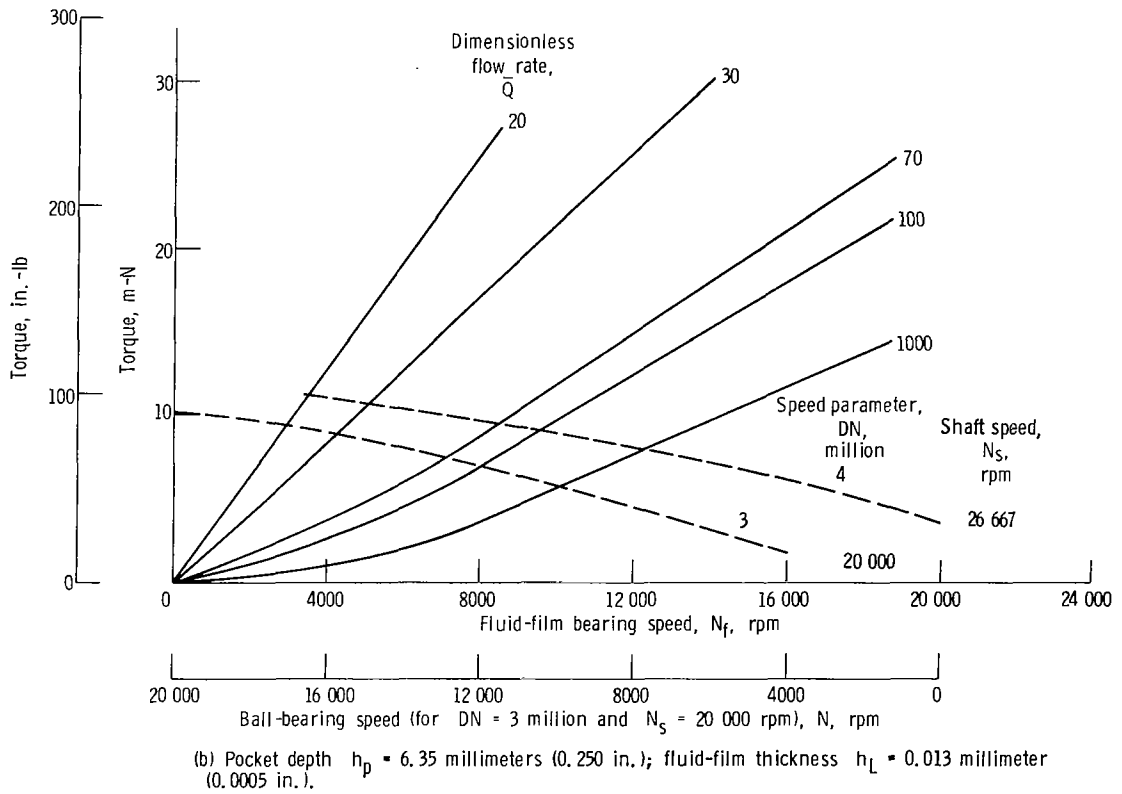
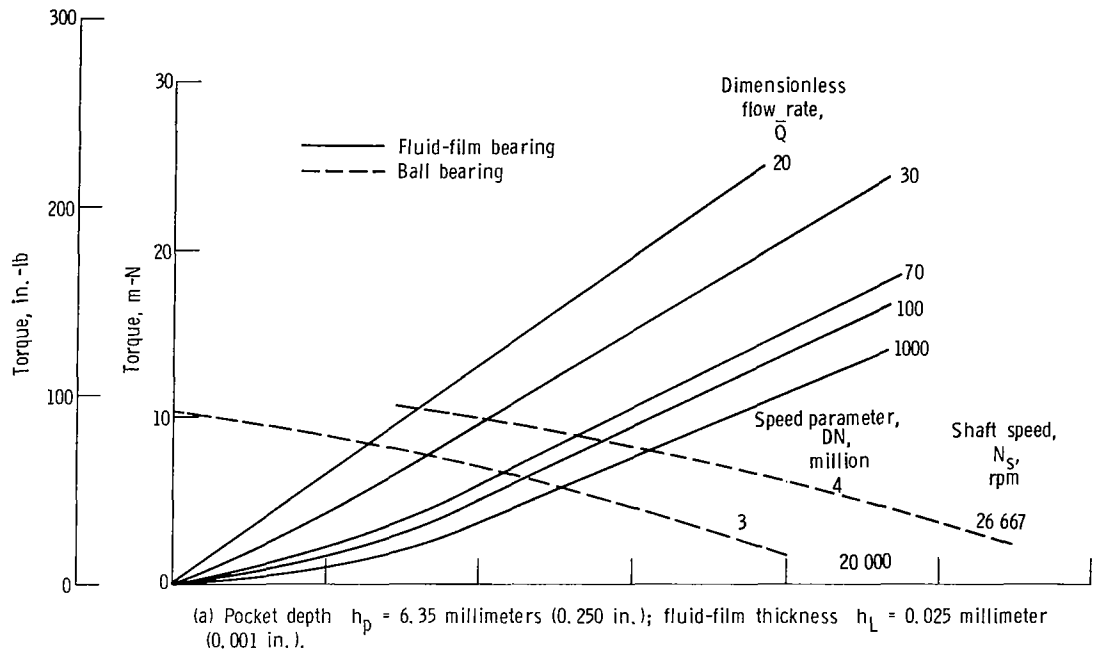


Figure 10. - Torque as a function of speed for a series-hybrid bearing. Thrust load  $F = 17\,800$  newtons (4000 lb).

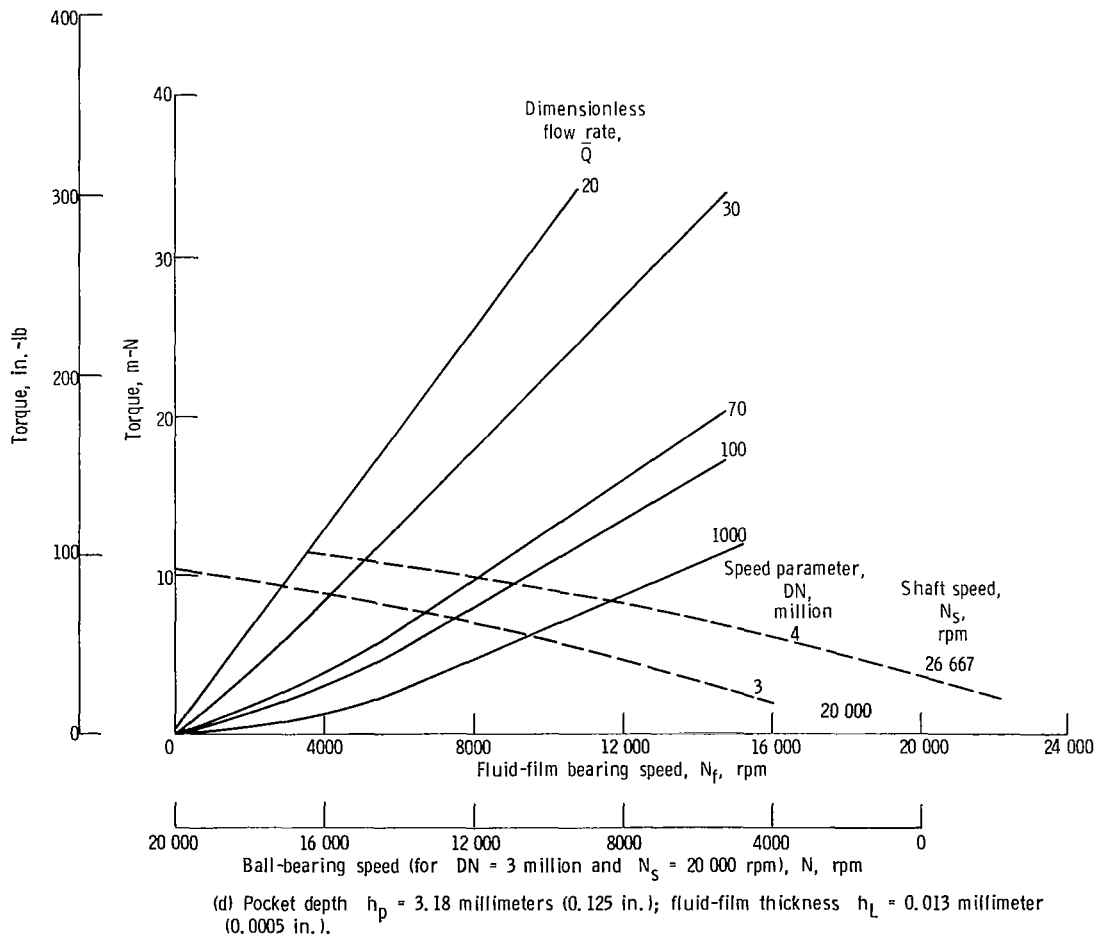
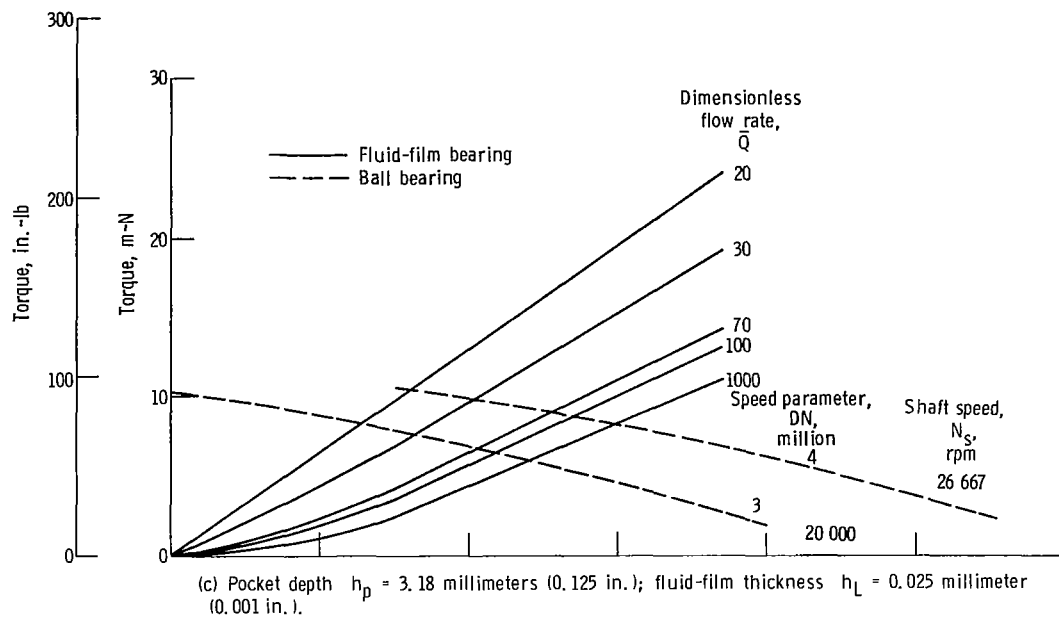


Figure 10. - Concluded.

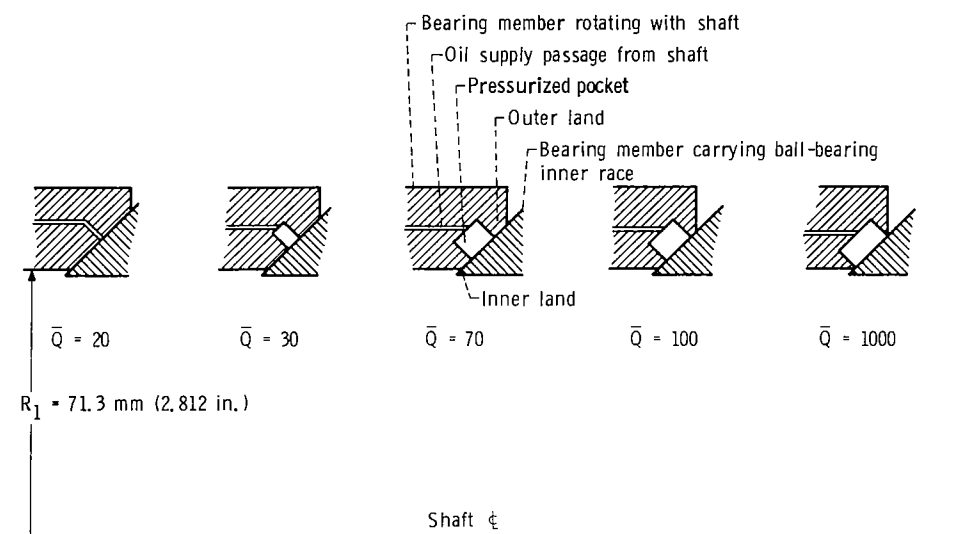
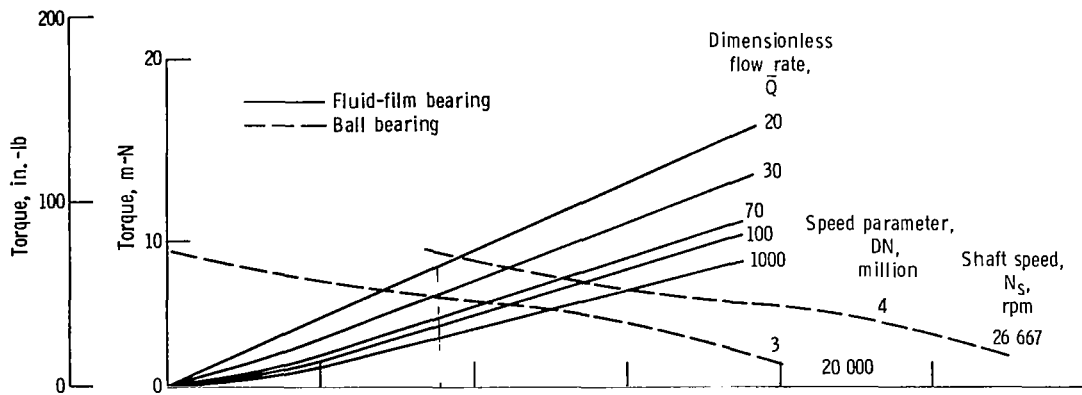
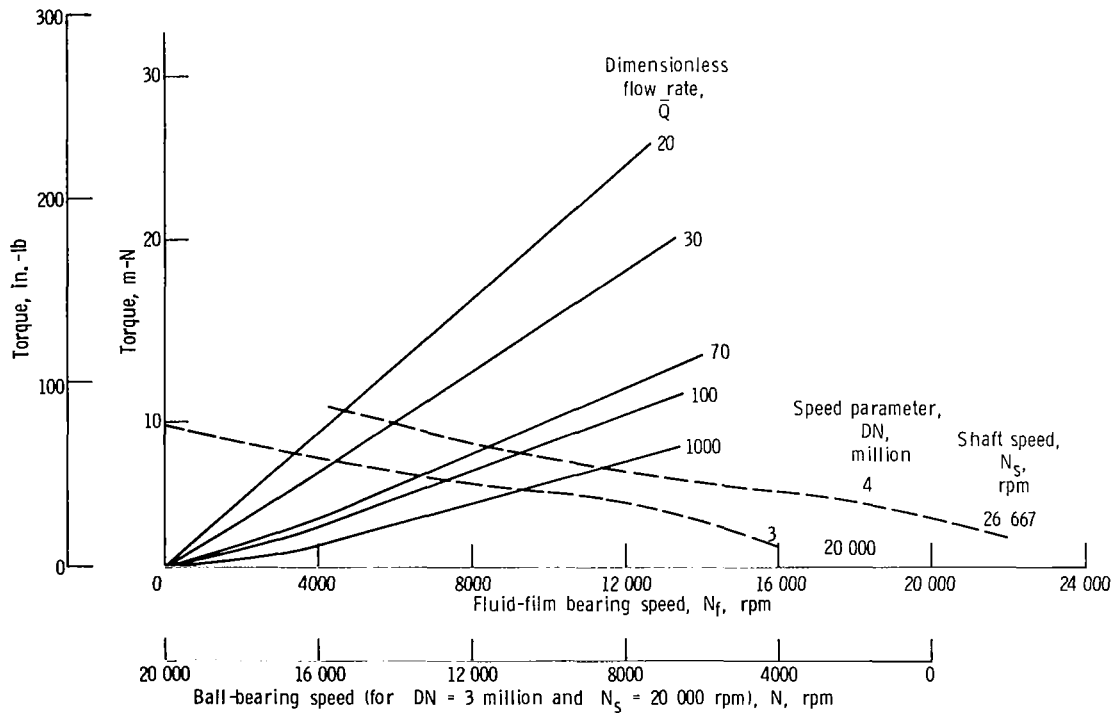


Figure 11. - Bearing proportions for values of dimensionless flow rate  $\bar{Q}$ . Inner radius of inner land  $R_1 = 71.3$  millimeters (2.812 in.).



(a) Fluid-film thickness  $h_L = 0.04$  millimeter (0.00159 in.).



(b) Fluid-film thickness  $h_L = 0.02$  millimeter (0.00079 in.).

Figure 12. - Torque as a function of speed for a series-hybrid bearing. Thrust load  $F = 4450$  newtons (1000 lb); pocket depth  $h_p = 3.18$  millimeters (0.125 in.).